



Effects of Varying Wind Angles and Increasing Concentration on Air Pollutant Dispersion from Cooling Towers to Urban Area using Computational Fluid Dynamics Software

*¹EHI-EROMOSELE, F; ²MACLAINE, A; ³OSADOLOR, AO; ⁴BILQEES, DM

^{*1,3}Department of Mechanical Engineering, University of Benin, Nigeria.

^{2,4}Department of Sustainable Engineering, Nottingham Trent University, United Kingdom.

*Corresponding Author Email: festus.ghi-eromosele@uniben.edu

Other Authors Email: allan.maclaine2018@my.ntu.ac.uk; alexander.osadolor@uniben.edu; bilqees.durosinmimustapha2021@my.ntu.ac.uk

ABSTRACT: Managing and improving the air quality across urban areas can be achieved by studying the transport behaviour of air pollutants. In this work, the effects of varying wind angles and increasing concentration on air pollutant dispersion from cooling towers to urban area were investigated using computational fluid dynamics (CFD) software; OpenFOAM and the modified k- ω SST turbulence closure to acquire the steady-state flow field based on Reynolds Averaged Navier-Stokes Equation (RANS) approach. The results showed that varying the wind direction for the wind velocity profile from (1 0 0) to (Cos30 0 Sin30) and (Cos45 0 Sin45) affected the pollution dispersion across the urban area with the worst scenario being (1 0 0). In addition, reducing the diffusivity constant (Dt), thus increasing the pollution concentration, from 0.02 to 0.001 increased the pollution transport across the urban area considerably. This research shows the benefit of applying CFD approach toward managing the challenges of air pollution dispersion.

DOI: <https://dx.doi.org/10.4314/jasem.v26i7.7>

Open Access Article: (<https://pkp.sfu.ca/ojs/>) This an open access article distributed under the Creative Commons Attribution License (CCL), which permits unrestricted use, distribution, and reproduction in any medium, provided the original work is properly cited.

Impact factor: <http://sjifactor.com/passport.php?id=21082>

Google Analytics: <https://www.ajol.info/stats/bdf07303d34706088ffffbc8a92c9c1491b12470>

Copyright: © 2022 Ehi-Eremosele *et al*

Dates: Received: 16 June 2022; Revised: 07 July 2022; Accepted: 17 July 2022

Keywords: Pollution dispersion; computational fluid dynamics; Reynolds Equation; Navier-Stokes Equation; Turbulence.

Air Pollution dispersion involves the pathway followed by pollutants (particulates, aerosols, biological molecules, or other harmful materials) introduced into the atmosphere through natural or anthropogenic sources thus resulting in damage to the natural environment, disease outbreaks, and human death (Brusseau *et al.*, 2019). The dispersion of these plumes has posed a primary concern to the governmental environmental protection agencies from around the world. Several computational fluid dynamics (CFD) models have been introduced in modelling the transport characteristics of air pollutants and these include box models, gaussian models, dense gas models, lagrangian models, and eulerian models. While the first three represent the older models, the last two have gained popularity in recent years (Srivastava and Sinha 2004; Leelőssy *et al.*, 2014). However, the major difference between the lagrangian and eulerian models is that while the former traces the trajectories of the pollution plumes and computes the motions as a

random walk using a moving reference frame, the latter uses a fixed three-dimensional Cartesian grid as a reference frame. This is achieved by observing a fixed grid as the plume passes by (Camelli *et al.*, 2006; Leelőssy *et al.*, 2014). These dispersion models estimate the concentration of air pollutants emitted from sources such as vehicular traffic, accidental chemical releases, or industrial plants. They also can help in predicting future concentrations for any given scenario. The CFD process can be divided into pre-processing, solver and the postprocessing. Nevertheless, CFD for industrial and environmental flow uses two main approaches to simulate the transport and dispersion of the pollution in an urban area and these include Large Eddy Simulation (LES) and Reynolds Averaged Navier-Stokes Equation (RANS) (Gao *et al.*, 2018; Baker *et al.*, 2019). RANS solves the time-averaged continuity and momentum equations by introducing an eddy-viscosity to compute the Reynolds stresses, thus simplifying the problem

*Corresponding Author Email: festus.ghi-eromosele@uniben.edu

into the solutions of two additional transport equations. Its computational resource requirement is only a small fraction of that required by LES and Direct Numerical Simulation (DNS) thus its preference for most industrial CFD applications (Straatman and Martinuzzi 2002; Pontiggia *et al.* 2010; Ye *et al.*, 2021). These eddy-viscosity RANS models include the Spalart-Allmaras model, the $k-\epsilon$ model, the $k-\omega$ model, the $k-\omega$ SST model, etc. The $k-\omega$ model is more accurate than $k-\epsilon$ model in the near wall layers and has been successfully applied for moderate pressure flow. However, the former fails for flows with pressure-induced separation compared to the latter and its sensitivity to the value of ω in the freestream outside the boundary layer limits its application as a standard scale equation. These drawbacks are the main motivation for the development of $k-\omega$ SST model which blends the original $k-\omega$ model (near the wall) with the $k-\epsilon$ model (away from the wall) (Menter *et al.*, 2003; Versteeg and Malalasekera 2007). Many studies show the dispersion of these pollutants and their transport characteristics using several available models. (Gao *et al.*, 2018) studied short episodes of local pollution dispersion using the open-source geometry and mesh generator SALOME and the CFD code code_Saturne. Results showed that the porous volume (simulated as tall trees) induced a drag force to the air flowing through it. In addition, the wind velocity and air temperature simulation agreed with the measurements obtained from a fixed station set up. In addition, increasing the height of the anti-noise walls as described in the two scenarios did not improve the neighbourhood air quality. (Chu *et al.*, 2005) studied the dispersion characteristics for different wind speeds and wind directions. The GIS software (ArcView 3.2a) was used to extract the building coordinates while the geometric simulation was modelled using the CFX5.5. (Shen *et al.*, 2017) investigated the relationship between flow patterns and dispersion process for different plan area densities, through a Large Eddy Simulation (LES), for the passive scalar in the turbulent boundary layer over an urban space under neutral and stable stratification. Results showed that the spread of the plumes reduced, and the temporal fluctuation decreased under stable stratification. (Balczó *et al.*, 2005) studied the effect of wind direction on the change of the annual mean concentration level, due to the construction of a new city, using the CFD code Microscale Flow and Dispersion Model (MISKAM) and FLUENT for its simulation. Result showed that MISKAM code agreed with calculated concentration to Wind Tunnel (WT) data but with significant differences at some wind directions. (Camelli *et al.*, 2006) studied the flow field inside an urban layout, incorporating the transport and

dispersion of passive scalar using the Eulerian framework through the CFD model called FEFLO-URBAN. The atmospheric flow was simulated using Very-Large Eddy Simulation (VLES). Results showed mesh resolution fine enough to capture very large eddies. The effects of the tall building (Chimney effect) and the relation between wind direction and street concentration for the lateral dispersion of the released materials were conducted. (Guo *et al.*, 2020) studied the effects of atmospheric stability on the flow structures and near-field plume dispersion in an urban-like environment under unstable, neutral, and stable atmospheric stratification using the steady RANS methodology. Scenarios of both perpendicular and oblique wind directional conditions were observed. Results showed that intense thermal turbulence enhanced the vortex intensity and plume dilution under unstable conditions. While the vertical profile of the streamwise velocity decreased by the obstacles thus increasing the concentration level and pollution spread due to weak turbulence motion under the stable condition. (Wang *et al.*, 2021) studied the effects of trees on airflow and pollution dispersion in urban canyons using a fine tree model for the numerical simulation of the airflow at varying inflow wind velocities. However, this research was aimed at determining the effects of varying wind angles and increasing concentration on air pollutant dispersion from cooling towers to urban area were investigated using computational fluid dynamics (CFD) software; OpenFOAM and modified $k-\omega$ SST turbulence closure to acquire the steady-state flow field based on Reynolds Averaged Navier-Stokes Equation (RANS) approach.

MATERIALS AND METHODS

The dispersion of pollution in an urban area is simulated by set of mass and momentum conservation equations. The flow is modelled as three-dimensional, turbulence, incompressible, and Newtonian flow, with a constant density in the computational domain. In this simulation, the modified $k-\omega$ SST model is applied to acquire the steady-state flow field based on the steady RANS approach.

Numerical Method: The Gaussian-linear finite volume scheme is applied for the spatial discretisation through OpenFOAM to solve the governing equations (1) to (5) subject to respective boundary conditions. Euler scheme is applied for the time advancement. The fluid property; ν_t , refers to the turbulent (eddy) viscosity. The Reynold's number, Re , is the ratio of convective force to viscous forces, which influences the fluid flow features within the channel. The governing equations follow a non-linear partial differential equation written as follows (Menter *et al.*, 2003):

$$EHI-EROMOSELE, F; MACLAINE, A; OSADOLOR, AO; BILQEES, DM$$

Continuity equation:

$$\frac{\partial(u)}{\partial x} + \frac{\partial(v)}{\partial y} + \frac{\partial(w)}{\partial z} = 0 \tag{1}$$

x-momentum equation:

$$\frac{\partial(u)\langle u \rangle}{\partial x} + \frac{\partial(u)\langle v \rangle}{\partial y} + \frac{\partial(u)\langle w \rangle}{\partial z} = -\frac{1}{p} \frac{\partial(p)}{\partial x} + \frac{\partial}{\partial x} \left[(v + v_t) \left(\frac{\partial(u)}{\partial x} + \frac{\partial(u)}{\partial x} \right) \right] + \frac{\partial}{\partial y} \left[(v + v_t) \left(\frac{\partial(u)}{\partial y} + \frac{\partial(v)}{\partial x} \right) \right] + \frac{\partial}{\partial z} \left[(v + v_t) \left(\frac{\partial(u)}{\partial z} + \frac{\partial(w)}{\partial x} \right) \right] \tag{2}$$

y-momentum equation:

$$\frac{\partial(u)\langle u \rangle}{\partial x} + \frac{\partial(u)\langle v \rangle}{\partial y} + \frac{\partial(u)\langle w \rangle}{\partial z} = -\frac{1}{p} \frac{\partial(p)}{\partial y} + \frac{\partial}{\partial x} \left[(v + v_t) \left(\frac{\partial(v)}{\partial x} + \frac{\partial(u)}{\partial y} \right) \right] + \frac{\partial}{\partial y} \left[(v + v_t) \left(\frac{\partial(v)}{\partial y} + \frac{\partial(v)}{\partial y} \right) \right] + \frac{\partial}{\partial z} \left[(v + v_t) \left(\frac{\partial(v)}{\partial z} + \frac{\partial(w)}{\partial y} \right) \right] \tag{3}$$

z-momentum equation:

$$\frac{\partial(u)\langle u \rangle}{\partial x} + \frac{\partial(u)\langle v \rangle}{\partial y} + \frac{\partial(u)\langle w \rangle}{\partial z} = -\frac{1}{p} \frac{\partial(p)}{\partial z} + \frac{\partial}{\partial x} \left[(v + v_t) \left(\frac{\partial(w)}{\partial x} + \frac{\partial(u)}{\partial z} \right) \right] + \frac{\partial}{\partial y} \left[(v + v_t) \left(\frac{\partial(w)}{\partial y} + \frac{\partial(v)}{\partial z} \right) \right] + \frac{\partial}{\partial z} \left[(v + v_t) \left(\frac{\partial(w)}{\partial z} + \frac{\partial(w)}{\partial z} \right) \right] \tag{4}$$

Limiters:

$$v_t = \frac{a_1 k}{\max(a_1 \omega; \Omega F_2)} \tag{5}$$

Transport equation for the pollution concentration (Versteeg and Malalasekera 2007) is:

$$\frac{\partial(c)\langle u \rangle}{\partial x} + \frac{\partial(c)\langle v \rangle}{\partial y} + \frac{\partial(c)\langle w \rangle}{\partial z} = \frac{\partial}{\partial x} \left[(D + D_t) \left(\frac{\partial(c)}{\partial x} \right) \right] + \frac{\partial}{\partial y} \left[(D + D_t) \left(\frac{\partial(c)}{\partial y} \right) \right] + \frac{\partial}{\partial z} \left[(D + D_t) \left(\frac{\partial(c)}{\partial z} \right) \right] \tag{6}$$

Where: D_t (turbulent diffusivity) $\approx v_t$; $C \equiv$ mass concentration $\equiv \frac{\delta m_{species}}{\delta m_{total}}$

Results showed that the pollutant concentration increased significantly in the presence of trees and with increasing inflow velocity.

Geometry and Mesh Generation: The channel is modelled as a lengthwise rectangular prism with coordinate vertices (0 1 2 3 4 5 6 7) corresponding to (0 0 -2), (12 0 -2), (12 4 -2), (0 4 -2), (0 0 2), (12 0 2), (12 4 2) and (0 4 2) respectively. The boundary layers include inlet face (0 4 7 3), outlet face (1 5 6 2), far side faces (0 1 2 3), (4 5 6 7), (2 6 7 3) and wall face (0 1 5 4).

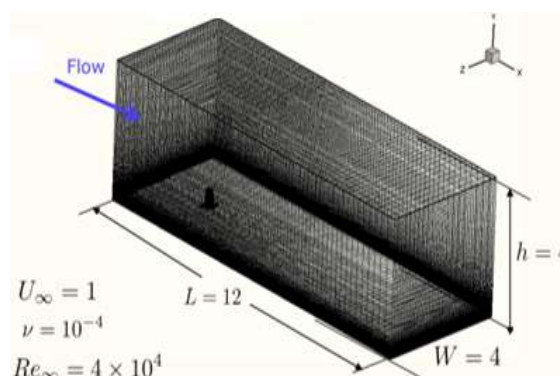


Fig 1: Turbulent Channel Mesh Geometry

Figure 1 below shows the turbulent channel mesh geometry with incorporated grip points. X-grid contains 120 grid points for its entire length (of two equal sections of length 6m) and it is spaced uniformly for the first half of the length and stretched for the remaining half by a stretching factor of 4. Y-grid has 80 grid points with a stretching factor of 1. Z-grid has 40 grid points spaced uniformly.

Computational Package: OpenFoam was used as the computational package for the CFD simulation. This is done after the software freeCAD is used for the design of the towers and the buildings meshed and integrated into the grid with the data set from table 1. Within the OpenFoam computational package, the command simpleFoam is applied as the CFD solver to create data

points within the domain across a determined time-period with a selected interval. The command scalarTransportFoam was also used to create data

points within the selected domain to determine the transport characteristics of pollution dispersion.

Table 1: FreeCAD geometry dimensions for towers and buildings

	Position					Dimension				
	Angle(°)	axis	x(mm)	y(μm)	z(mm)	L(mm)	W(mm)	h(mm)	r1(mm)	r2(mm)
Tower1	360	(1,0,0)	2	-50	0			0.5	0.1	0.15
Tower2	360	(1,0,0)	2	-50	-0.5			0.5	0.1	0.15
Tower3	360	(1,0,0)	2.05	-50	0.5			0.5	0.1	0.15
Building1	-90	(1,0,0)	8	-50	-0.5	0.2	0.15	0.7		
Building2	-90	(1,0,0)	8.5	-50	0.5	0.3	0.2	0.6		
Building3	-90	(1,0,0)	9	-50	0	0.15	0.15	0.8		
Building4	-90	(1,0,0)	8	-50	0	0.5	0.2	0.65		
Building5	-90	(1,0,0)	9	-50	0.5	0.15	0.2	0.9		
Building6	-90	(1,0,0)	9	-50	-0.5	0.15	0.2	0.9		
Building7	-90	(1,0,0)	8.5	-50	0	0.3	0.2	1		

Transport Properties and Boundary Conditions: To determine the effect of pollution concentration on the transport behaviour of pollution dispersion, the transport phenomenon is applied. This is achieved by applying the convergent values of u , v , and w from the RANS equations (1) to (5) to solve for the parameter ‘ c ’ (treated as a passive and continuous, eulerian, scalar transport property) in equation (6). Boundary conditions for the scalar transport was set as represented by the component, T , in table 2 below. In addition, boundary conditions are set for $\langle u \rangle$, $\langle p \rangle$, ω , k , v_t for the momentum simulation as show in table 2 below. These boundary conditions determine the transport behaviour of the fluids in the domain over a period.

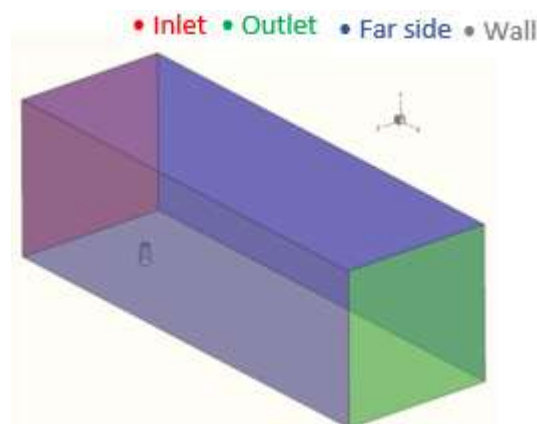


Fig 2: Channel Boundary Conditions

Table 2: Boundary conditions for pollution dispersion simulation

Boundary conditions	p	u	k	v_t	ω	T
Inlet	zerogradient	Fixed value (v)	Fixed value (0.01U∞^2)	Fixed value (U∞^3/h)	Fixed value (U∞/h)	Fixed value (0)
Outlet	Fixed value	zerogradient	zerogradient	zerogradient	zerogradient	zerogradient
Far side	zerogradient	zerogradient	zerogradient	zerogradient	zerogradient	zerogradient
Wall	zerogradient	noslip	Fixed value (0)	Fixed value (0)	Fixed value (100U∞/h)	zerogradient
Cooling Tower Top	zerogradient	Fixed value (v)	Fixed value (0)	Fixed value (0)	Fixed value (100U∞/h)	Fixed value (1)
Cooling tower side	zerogradient	noslip	Fixed value (0)	Fixed value (0)	Fixed value (100U∞/h)	zerogradient
Building	zerogradient	noslip	Fixed value (0)	Fixed value (0)	Fixed value (100U∞/h)	zerogradient

Grid Convergence: This is determined by plotting the variation of velocity against time for two probes on the channel profile at the same height but at different x-location. Then convergence is reached when the profile shows similar signals.

Alternatively, convergence can be determined from the paraFoam of the channel profile when no changes are observed by comparing the output profile for consecutive time steps.

RESULTS AND DISCUSSION

To demonstrate the effect of varying wind angles on pollution dispersion, different simulations were carried out by changing the wind direction according to scenarios 1 to 3 in table 3 and the boundary conditions for the channel far walls were modified accordingly. The effect of increasing the concentration of pollution from the towers on the transport behaviour was conducted by varying the

value of the pollution concentration from the towers as shown in scenario 4 in table 3.

Table 3: Table of runs for pollution dispersion

	Wind direction for u (xyz)	Far wall BC	Re	Pollution conc. (Dt)
Scenario 1	(1 0 0)	zerogradient	10000	0.02
Scenario 2	(Cos30 0 Sin30)	Fixed value (v)	10000	0.02
Scenario 3	(Cos45 0 Sin45)	Fixed value (v)	10000	0.02
Scenario 4	(1 0 0)	zerogradient	10000	0.001

Comparing the pollution dispersion for the U velocity profile for scenarios 1 to 3 in figure 3(a to c), figure 5(a to c), and figure 7(a to c) respectively, it was observed that increasing the wind direction reduced the pollution dispersion across the urban area with the least pollution dispersion in scenario 3. Figure 4, figure 6, and figure 8 show the scalar transport behaviour for scenario 1, scenario 2, and scenario 3 respectively. The effect of obstacles (buildings) on the pollution dispersion was demonstrated by placing two probes along the u velocity profile horizontally at positions $x=1$, away from the buildings, and at position $x=5$, close to the buildings. The graph showed that at distance $x=5$, the concentration of the pollution increased for all scenarios studied compared to the position $x=1$ as seen from the wavelength in figure 3(e), figure 5(e), and figure 7(e) as opposed to figure 3(d), figure 5(d), and figure 7(d). In addition, the graphs of the U velocity profile were compared for scenarios 1, 2, and 3 in figure 3(d), figure 5(e), and figure 7(e) respectively for position $x=5$ (that is, close to the building). It was observed that the pollution dispersion increased from 0 to height 0.8m for scenario 1, height 0.2 for scenario 2 and height 0.18 for scenario 3. This indicates that, increasing the value of the wind angle reduced the pollution dispersion across the urban area. From figure 4(e) below, the graph showed that the concentration of pollution dispersion at probe point ($x=5$) increased from 0 value on the wall (due to no Slip condition) to a peak value at $y=0.5$ (height of the cooling towers) and experienced a gradual decrease until it got to point at $y=1.8$ where its value again turned to 0. This was also observed in the graph for figures 6(e) and 9(e). The effect of increasing the pollution concentration on pollution dispersion was demonstrated by reducing the diffusivity constant (Dt), thus increasing the pollution concentration, from 0.02 in scenarios 1, 2, and 3 to 0.001 in scenario 4. The scalar transport profile shows an increase in the amount of pollution reaching the urban area as seen from figure 9(a to c) as compared to figure 3(a to c).

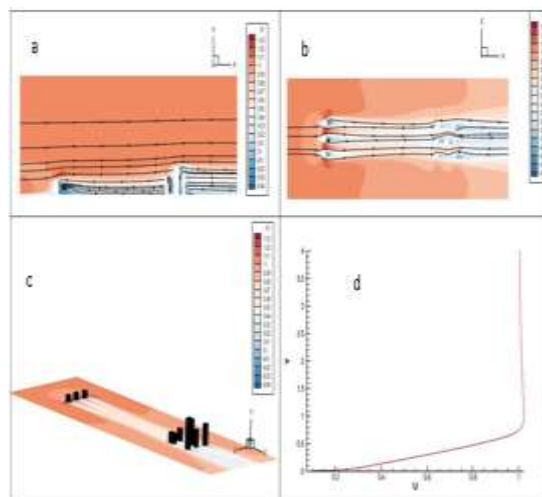


Fig 3: Pollution dispersion for scenario 1(a to c); graph of U velocity profile along horizontal passing through point ($x=5$)

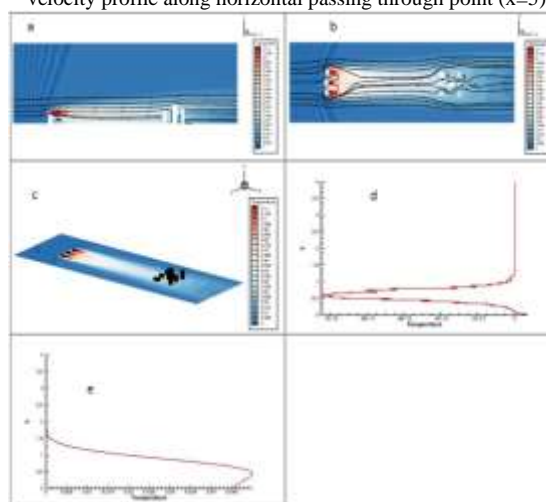


Fig 4: Scalar Transport for scenario 1(a to c); graph of pollution conc. (T) along horizontal passing through point ($x=1$)(d) and ($x=5$)(e)

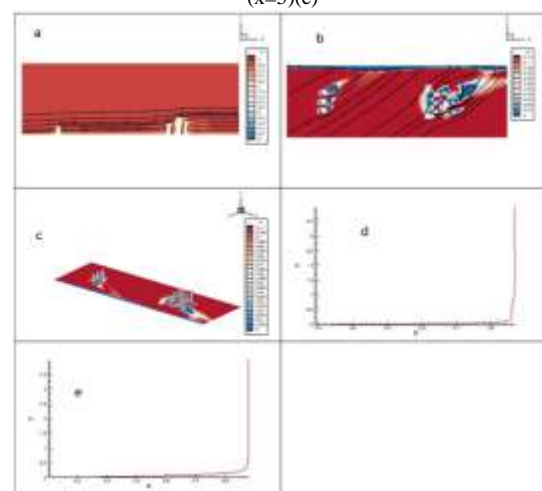


Fig 5: Pollution dispersion for scenario 2(a to c); graph of U velocity profile along horizontal passing through point ($x=1$)(d) and ($x=5$)(e)

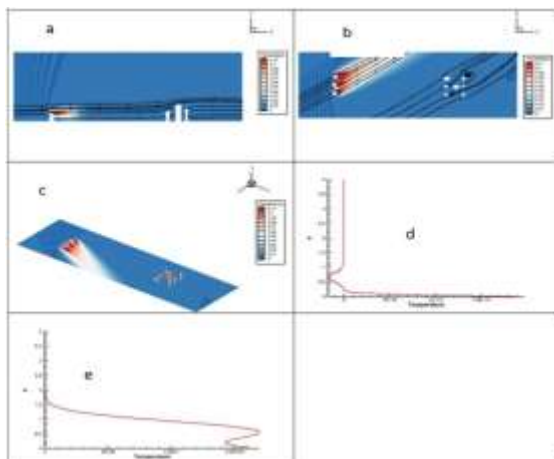


Fig 6: Scalar Transport for scenario 2(a to c); graph of pollution conc. (T) along horizontal passing through point (x=1)(d) and (x=5)(e)

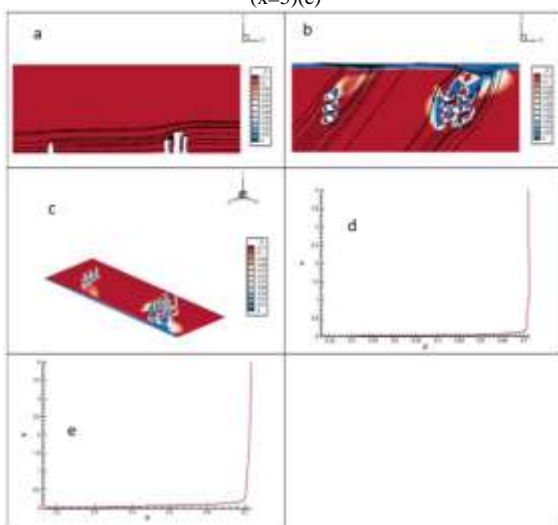


Fig 7: Pollution dispersion for scenario 3(a to c); graph of U velocity profile along horizontal passing through point (x=1)(d) and (x=5)(e)

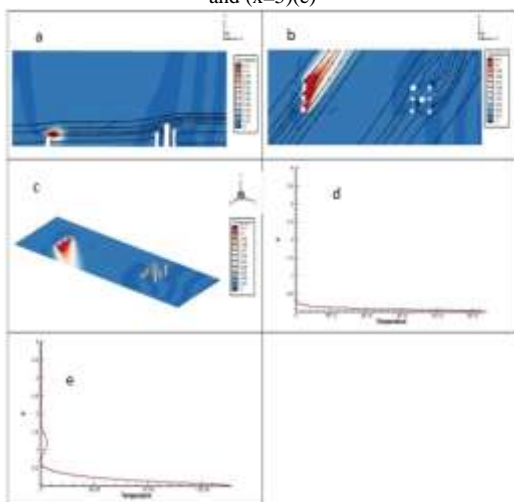


Fig 8: Scalar Transport for scenario 3(a to c); graph of pollution conc. (T) along horizontal passing through point (x=1)(d) and (x=5)(e)

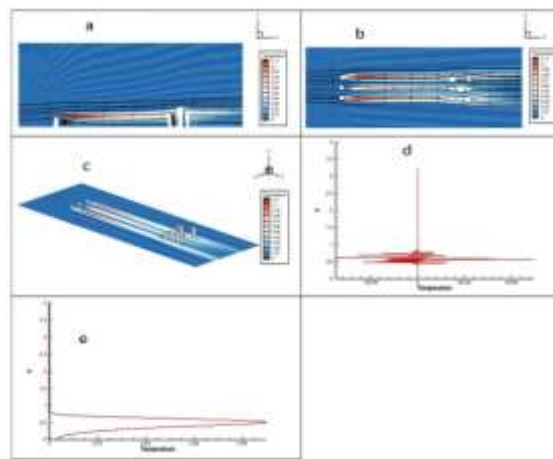


Fig 9: Scalar Transport for scenario 4(a to c); graph of pollution conc. (T) along horizontal passing through point (x=1)(d) and (x=5)(e)

Conclusion: The transport characteristics of pollution dispersion to an urban area have been investigated. This work evaluated the effect of varying wind angles on pollution dispersion and the effect of increasing the concentration of pollution from the towers on the transport properties. Increasing the pollution concentration from the towers increased the transport characteristics of the dispersed pollution considerably. This work has demonstrated the benefit of applying CFD simulation to determine pollution dispersion for varying input scenarios.

REFERENCES

Baker, C.; Johnson, T.; Flynn, D.; Hemida, H.; Quinn, A.; Soper, D; Sterling, M. (2019). *Train aerodynamics: fundamentals and applications*. Butterworth-Heinemann.

Balczó, M.; Faragó, T.; Lajos, T. (2005). Modelling urban pollution dispersion by using MISKAM. In *Proceedings der Konferenz microCAD*, pp.10-11.

Brusseau, M.L., Matthias, A.D., Comrie, A.C. and Musil, S.A., 2019. Atmospheric pollution. In *Environmental and Pollution Science*, pp. 293-309. Academic Press.

Camelli, F.; Lohner, R.; Hanna, S. (2006). VLES study of flow and dispersion patterns in heterogeneous urban areas. In *44th AIAA Aerospace Sciences Meeting and Exhibit*. pp.1419.

Chu, A.K.M.; Kwok, R.C.W.; Yu, K.N. (2005). Study of pollution dispersion in urban areas using Computational Fluid Dynamics (CFD) and

- Geographic Information System (GIS). *Environ. Modelling. Software*. 20(3). 273-277
- Gao, Z.; Bresson, R.; Qu, Y.; Milliez, M.; de Munck, C.; Carissimo, B. (2018). High resolution unsteady RANS simulation of wind, thermal effects and pollution dispersion for studying urban renewal scenarios in a neighborhood of Toulouse. *Urban Climate*. 23. 114-130.
- Guo, D.; Zhao, P.; Wang, R.; Yao, R.; Hu, J. (2020). Numerical simulations of the flow field and pollutant dispersion in an idealized urban area under different atmospheric stability conditions. *Process Safety. Environ. Protect*. 136. 310-323.
- Leelőssy, A.; Molnár, F.; Izsák, F.; Havasi, A.; Lagzi, I.; Mészáros, R. (2014). Dispersion modeling of air pollutants in the atmosphere: a review. *Open Geosci*. 6(3).257-278.
- Menter, F.R.; Kuntz, M.; Langtry, R. (2003). Ten years of industrial experience with the SST turbulence model. *Tubule. Heat. Mass. Transfer*. 4(1): 625-632.
- Pontiggia, M.; Derudi, M.; Alba, M.; Scaioni, M.; Rota, R. (2010). Hazardous gas releases in urban areas: Assessment of consequences through CFD modelling. *J. Hazard. Mat*. 176(1-3). 589-596.
- Shen, Z.; Cui, G.; Zhang, Z. (2017). Turbulent dispersion of pollutants in urban-type canopies under stable stratification conditions. *Atoms. Environ*. 156:1-14
- Srivastava, S.; Sinha, I.N. (2004). Classification of air pollution dispersion models: a critical review. In *Proceedings of National Seminar on Environmental Engineering with special emphasis on Mining Environment*.
- Straatman, A.G.; Martinuzzi, R.J. (2002). A study on the suppression of vortex shedding from a square cylinder near a wall. In *Engineering Turbulence Modelling and Experiments 5*, pp. 403-411. Elsevier Science Ltd.
- Versteeg, H.K.; Malalasekera, W. (2007). *An introduction to computational fluid dynamics: the finite volume method*. Pearson education.
- Wang, L.; Su, J.; Gu, Z.; Tang, L. (2021). Numerical study on flow field and pollutant dispersion in an ideal street canyon within a real tree model at different wind velocities. *Comp. Math. Applic*. 81:679-692.
- Ye, W.; Pan, Y.; He, L.; Chen, B.; Liu, J.; Gao, J.; Wang, Y.; Yang, Y. (2021). Design with modelling techniques. In *Industrial Ventilation Design Guidebook*, pp.109-183. Academic Press.